

# Orientation changes of the large-scale circulation in turbulent Rayleigh-Bénard convection

Eric Brown, Alexei Nikolaenko, and Guenter Ahlers

Department of Physics and QUEST, University of California, Santa Barbara, CA 93106  
(Dated: May 24, 2019)

We present measurements of the orientation  $\theta(t)$  of the large-scale circulation (LSC) of turbulent Rayleigh-Bénard convection in cylindrical cells of aspect ratio 1.  $\theta(t)$  undergoes irregular rotation. It contains reorientation events through angles  $\pi$  with a monotonically decreasing probability distribution  $p(\theta)$ , i.e. there is no dominant value of  $\theta$  and small  $\theta$  are more common than large ones. The reorientations have Poissonian statistics in time. The amplitude  $\Delta\theta$  of the LSC and azimuthal rotation rate  $\dot{\theta}$  for reorientations are related by a power law, with smaller  $\Delta\theta$  at larger  $\dot{\theta}$ .

PACS numbers: 47.27.-i, 05.65.+b, 47.27.Te

A major component of turbulent Rayleigh-Bénard convection [1, 2, 3] (RBC) in a fluid heated from below is the emission of hot (cold) volumes of fluid known as "plumes" from bottom (top) thermal boundary layers. These plumes are carried by, and by virtue of their buoyancy in turn drive, a large-scale circulation (LSC) [4, 5, 6, 7, 8, 9] known as the "mean wind". For cylindrical samples of aspect ratio  $D=L/1$  ( $D$  is the sample diameter and  $L$  the height) the LSC is a circulation in a near-vertical plane with up-flow and down-flow on opposite sides close to the side wall. An interesting aspect of the LSC observed by others is that it can spontaneously and erratically change directions [10, 11, 12, 13], either by an azimuthal rotation of the entire structure without much change of the flow speed, or by reversing its flow direction without much rotation of the circulation plane. The rotation was observed in experiments [11]; but to our knowledge the near-instantaneous reversal so far had been demonstrated only in numerical simulations of a two-dimensional system [10] and in a dynamical-systems model of the phenomenon [14]. Thus, for the most part the rotation and reversal in the LSC dynamics are still poorly understood. The phenomena are important for instance because they occur in natural convection of the Earth's atmosphere [15], and because they are responsible for changes in the orientation of the Earth's magnetic field that is a result of convection reversal in the outer core [16].

In this letter we describe experiments that shed new light on the nature of the reorientation of the LSC. We found that there is a broad spectrum of events leading to flow reorientation. At one extreme there is relatively slow rotation, over a time period of order ten turnover times  $T$  of the LSC, without a significant decrease of the circulation speed. At the other, there are near-instantaneous reversals that involve a vanishing of the flow speed followed by a re-initiation of the circulation with different angular orientations  $\theta$ . The new orientations correspond to a continuous range of angular changes  $\Delta\theta$ , including the "reversal" involving  $\Delta\theta/2\pi=1/2$  (we measure  $\theta$  in units of  $2\pi$ , i.e. of revolutions) that was seen in two-

dimensional simulations [10] (where only this is possible), favored in the interpretation of some experiments [13], and contained in a recently developed model [14]. As seen by others [13], the temporal succession of reorientation events had a Poissonian distribution, suggesting that successive events are independent of each other.

The experiments cover the range  $3 \cdot 10^8 < R < 10^{11}$  of the Rayleigh number  $R = gTL^3/\nu\alpha T$  ( $g$  is the isobaric thermal expansion coefficient,  $\nu$  the acceleration of gravity,  $T$  the applied temperature difference,  $\alpha$  the thermal diffusivity, and  $\nu$  the kinematic viscosity). The Prandtl number was  $\Pr = 4.4$ . Two cylindrical samples with aspect ratio  $D/1$  were used and are the medium and large sample described in detail elsewhere [17]. Both had circular copper top and bottom plates and a plexiglas side wall. The medium (large) sample had  $D = 24.81$  (49.67) cm and  $L = 24.76$  (50.61) cm. Each was filled with water at a mean temperature  $T_m = 40$  C. Eight blind holes were drilled from the outside into the side walls. They were equally spaced azimuthally in the horizontal mid-plane of the samples. Thermistors were placed into them so as to be within 0.07 cm of the fluid surface. They detected the location of the up-flow (down-flow) of the LSC by indicating a relatively high (low) temperature, but did not perturb the flow structure in the fluid. We made measurements with a sampling period  $\Delta t = 6$  seconds, and at the function  $T_i = T_0 + \Delta T \cos(i - \theta_0)$ ;  $i = 0; \dots; 7$ , separately at each time step, to the eight temperature readings. Here  $\Delta T$  is a measure of the amplitude of the LSC and  $\theta_0$  is the angular orientation of the plane of circulation. Typically the uncertainties were about 13% for  $\Delta T$  and 0.02 for  $\theta_0$ . We calculated the angular change  $\Delta\theta = \theta(t + \Delta t) - \theta(t)$  and the azimuthal rotation rate  $\dot{\theta} = \Delta\theta/\Delta t$ .

In Fig. 1a we show a long time series of  $\theta$  from the large cell and for  $R \approx 10^{11}$ . It covers a period of nine days. In this example, on average one sees net rotation, at a rate of about one revolution per day in the clockwise direction when viewed from above. Net rotation was observed also by Sun et al. [18], but in the counter-clockwise direction.

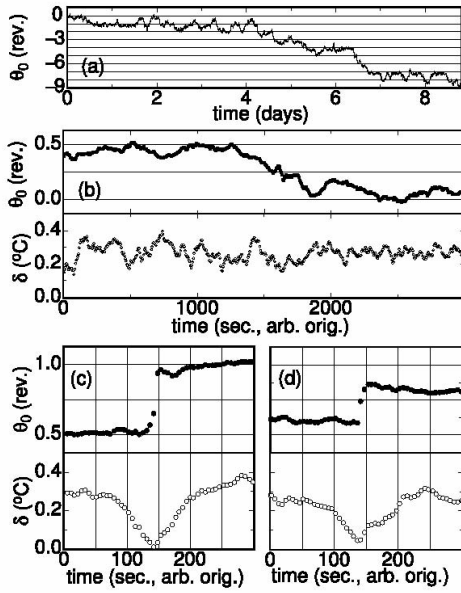


FIG. 1: Time series of the orientation  $\theta_0$  (in revolutions) and of the amplitude  $\delta$  (in  $^\circ$ ). (a): long time series of  $\theta_0$  from the large sample for  $R = 9.4 \cdot 10^{10}$ . (b) to (d): time series during reorientations from the medium sample for  $R = 1:1 \cdot 10^0$  for (b): a rotation; (c): a reversal; and (d): a half-reversal.

Hidden away in time series like that in Fig. 1a are numerous reorientation events. A few examples for the medium cell and  $R = 1:1 \cdot 10^0$  are shown in Figs. 1b to d (for this case  $T = 49$ s). Figure 1 (b) shows a net angular change  $\Delta\theta = 1/2$  over a period of about  $10T$ , similar to an event reported in Ref. [11]. The reversal time much larger than  $T$  indicates a relatively slow rotation of the LSC orientation. Throughout this event  $\delta$  is seen to remain non-zero.

Figure 1 (c) also shows an angular change of approximately half a revolution, but the change occurred in a fraction of  $T$ . Here  $\delta$  decreased for about one turnover time before the reversal, reached approximately zero during the reversal, and then increased for about another  $T$ . One sees that the mean wind gradually slowed to a stop, reversed direction, and gradually sped up again without significant rotation of the plane of circulation. This is the mechanism favored by Sreenivasan et. al. [13] in the interpretation of their data. Presumably it would prevail in systems where the rotational invariance is broken, either by imperfections of a nominally cylindrical sample or by a deliberate other choice of the geometry such as a square horizontal cross section. As we shall see below, in our system such events are relatively rare.

In Fig. 1 (d) the plots are qualitatively similar to (c). As in (c), the vanishing of  $\delta$  indicates that the LSC stopped, but when it re-started, it assumed an orienta-

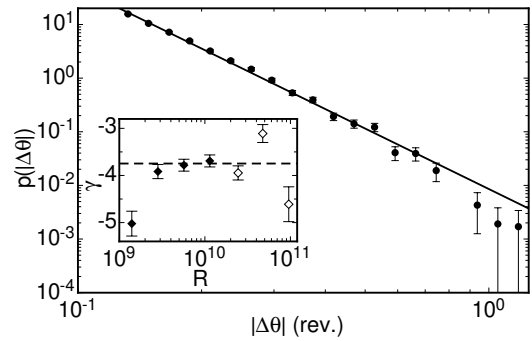


FIG. 2: Probability distribution of the angular change  $p(\Delta\theta)$  for reorientations. Solid circles: All data from the medium sample. Solid line: power-law fit to the data. Inset: power-law exponent versus  $R$  for the medium cell (solid diamonds) and large cell (open diamonds). Dashed line: the value of  $\gamma$  from the fit to all data. Note that reversals with  $\Delta\theta = 0.5$  are relatively rare with  $p(\Delta\theta = 1/2) \approx 0.1$ , implying that only about 1% of the events correspond e.g. to  $\Delta\theta = 1/2 \approx 0.5$ .

tion that differed by  $\Delta\theta = 1/4$  from the original one. Many other values of  $\Delta\theta$  were observed, indicating that there is a larger class of phenomena with a continuous distribution of  $\Delta\theta$ .

In order to automatically identify members of the expected large spectrum of reorientation events, we required reorientations to satisfy two criteria. First, the magnitude of the net angular change in orientation  $\Delta\theta_j$  over a set of successive data points for  $\theta_0$  had to be greater than  $\Delta\theta_{min}$ . Second, the magnitude of the net average azimuthal rotation rate  $\langle \dot{\theta} \rangle = \Delta\theta_j / \Delta t_j$  over that set had to be greater than  $\dot{\theta}_{min}$ . Here  $\Delta t_j$  is the duration of the reorientation. Often there were multiple overlapping sets that satisfied these requirements. Then the set with the maximum local quality factor  $Q_n = \Delta\theta_j^n / (\Delta t_j)^n$  was chosen as the reorientation. For  $0 < n < 1$ ,  $Q_n$  represents a compromise between choosing the maximum angular change ( $Q_0$ ) or the maximum rotation rate ( $Q_1$ ). Any adjacent points to the chosen set were also included if the rotation rate for the additional range was greater than  $\dot{\theta}_{min}$  and of the same sign as the reorientation. Mostly we used the parameters  $\Delta\theta_{min} = 0.125$ ,  $\dot{\theta}_{min} = 0.1/T$ , and  $n = 0.25$ ; but since all three are arbitrary, we did the analysis over the ranges  $1/64 \leq \Delta\theta_{min} \leq 0.25$ ,  $0.0125 \leq \dot{\theta}_{min} \leq 0.2/T$ , and  $0 \leq n \leq 1$  to confirm that the results are not sensitive to the choice. For  $\Delta\theta_{min}$  and  $\dot{\theta}_{min}$ , the smallest values used were close to the noise level of the data, and above the largest values too few reorientations were counted to yield useful statistics. The qualitative conclusions of the analysis did not change with different parameter values. However, some of the quantitative values changed. This will be mentioned as it is appropriate.

An obvious feature of reorientations is the angular change  $\Delta\theta$ . All of the reorientations found for the

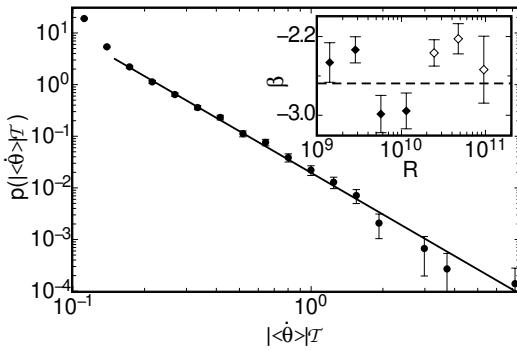


FIG. 3: The probability distribution  $p(|\dot{h}|T)$  of the azimuthal rotation rate for reorientations. Solid circles: data from the medium sample. Solid line: power-law fit to the data. The inset shows the power-law exponent  $\beta$  versus  $R$  for the medium cell (solid diamonds) and large cell (open diamonds). Dashed line: the value of  $\beta$  from the fit to all data.

medium sample were sorted into bins according to  $|\dot{h}|$ , regardless of the Rayleigh number  $R$ . The probability distribution  $p(|\dot{h}|)$  is shown in Fig. 2 with relative errors equal to the inverse square root of the number of reorientations in each bin. Fitting all data for  $p(|\dot{h}|)$  to a power law in the range  $|\dot{h}| \in [0.125, 1]$  yielded  $p(|\dot{h}|) \propto |\dot{h}|^{-\beta}$ , with  $\beta = 3.75 \pm 0.04$ . The same analysis was done also for reorientations at various fixed  $R$ . These probability distributions also could be fitted by power laws, with the resulting  $\beta$  values shown for each  $R$  in the inset of Fig. 2. One sees that the distribution was, within our resolution, independent of  $R$ . The power-law exponents were approximately constant over large ranges of the reorientation definition parameters; however they could vary by a factor of 2 for extreme values of the parameters. Qualitatively in all cases, the distribution was consistent with a power law for  $|\dot{h}| \in [0.125, 1]$  with a large negative  $R$ -independent exponent. The major qualitative conclusions are that there is a continuous distribution of  $|\dot{h}|$ , that smaller reorientations are much more common than larger ones, and that there is no characteristic reorientation size.

The azimuthal rotation rate  $h_i$  (where  $h_i$  indicates an average over the duration  $t$  of a given reorientation) was characterized by the same method as that used for  $|\dot{h}|$ . All of the reorientations from the medium sample were sorted into bins according to  $h_i T$  (the rotation rate was multiplied by  $T$  to make it dimensionless). The probability distribution  $p(h_i T)$  is plotted in Fig. 3. Fitting a power law to the data in the range  $h_i T \in [0.15, 1]$  yielded  $p(h_i T) \propto (h_i T)^{-\beta}$ , where  $\beta = 2.85 \pm 0.05$ . Again the same analysis was also done for individual values of  $R$ , and  $\beta$  is shown for each in the inset of Fig. 3. As for  $|\dot{h}|$ ,  $\beta$  can vary by about a factor of 2 with extreme values for the reorientation definition parameters, but the qualitative results are unchanged. The probability distribution  $p(h_i T)$  is described well by a power law with a large

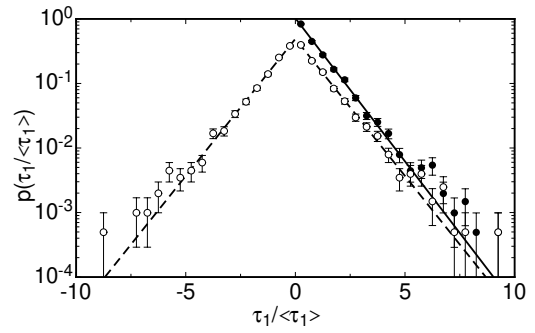


FIG. 4: Solid circles: probability distribution  $p(\tau_1 = h_i T)$  of the time intervals  $\tau_1$  between successive reorientations with a fit by an exponential function (solid line). Open circles: the probability distribution  $p(\tau_1 = h_i T)$  of the difference between successive intervals with a fit by an exponential function (dashed line).

negative exponent that is within our resolution independent of  $R$ , showing that slower reorientations are much more common than faster ones, and that there is no characteristic rotation rate for reorientations. We note that the normalization by  $T$  results in a  $p(h_i T)$  essentially independent of  $R$ , even though  $T/R \propto R^{-0.46}$  [19].

Another aspect of reorientations is their distribution in time. All of the time intervals  $\tau_1$  between the  $i$ th and  $(i+1)$ th reorientations from the medium sample were sorted into bins according to the value of  $\tau_1$ . The probability distribution  $p(\tau_1 = h_i T)$  is shown in Fig. 4. The average time interval between reorientations  $h_i T$ , computed separately at each  $R$ , was approximately  $30T$ , but quantitatively depended on the definition of reorientations and on  $R$ . The probability distribution can be fitted by the function  $p(\tau_1 = h_i T) / \exp(-\tau_1 / (h_i T)_{i,0})$  with  $(h_i T)_{i,0} = 0.98 \pm 0.02$ . This is consistent with a Poissonian distribution, which would correspond to an exponential function with  $(h_i T)_{i,0} = 1$ .

The Poissonian nature of reorientations can be seen further by considering the difference between successive time intervals. Thus,  $\tau_1 = \tau_{1,i+1} - \tau_{1,i}$  was sorted into bins according to  $\tau_1 = h_i T$  and the probability distribution  $p(\tau_1 = h_i T)$  is also plotted in Fig. 4. This distribution can be fitted by  $p(\tau_1 = h_i T) / \exp(-\tau_1 / (h_i T)_{1,1})$  with  $(h_i T)_{1,1} = 1.02 \pm 0.02$ . Again, for a Poissonian distribution  $(h_i T)_{1,1} = 1$ . The analysis in terms of  $\tau_1$  and  $\tau_1$  is consistent with that done by Sreenivasan et. al. [13] for "reversals" in their experiment that were counted very differently.

Next we consider the relationship between the amplitude  $h_i$  and the magnitude of the rotation rate  $|\dot{h}|$  for reorientations. All of the  $h_i$  from the medium sample were normalized by the average amplitude  $\langle h_i \rangle$  separately for each  $R$  and sorted into bins according to the value of  $h_i / \langle h_i \rangle$ . The average  $h_i$  of  $h_i$  in each bin as a function of  $|\dot{h}|$  is plotted in Fig. 5. The error bars are the

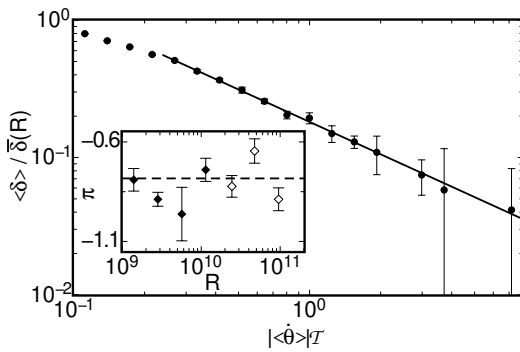


FIG. 5: The average  $\overline{h_i}(R)$  of the amplitude versus rotation rate  $|j-j|$  for reorientations (solid circles). The inset shows the exponent from the fit of  $\overline{h_i}(R) / (|j-j|)$  to the data for the medium cell (solid diamonds) and the large cell (open diamonds). Dashed line: the value of  $\alpha$  from the fit to all data.

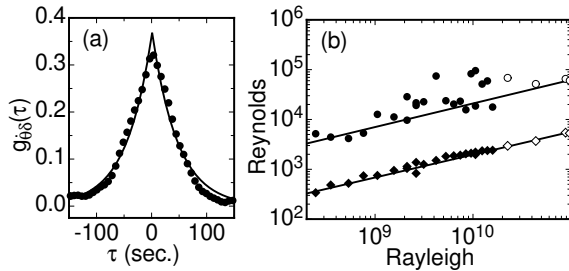


FIG. 6: (a): The negative cross-correlation  $g_{hh}(\tau)$  between the magnitude of the rotation rate  $|j-j|$  and the amplitude at  $R = 1:1 \cdot 10^0$  (solid circles) and a fit by an exponential function (solid line). (b): Reynolds numbers for the average  $g_{j0}$  [solid (open) circles] and width  $g_{j1}$  [solid (open) diamonds] of  $g_{hh}(\tau)$  for the medium (large) sample.

probable error of the mean for each bin. A power law fit in the range  $|j-j| = 0.24$  yielded  $[\overline{h_i}(R)] / (|j-j|)$  with  $\alpha = 0.78 \pm 0.03$ . The values of  $\alpha$  in the inset of Fig. 5 show that, with the normalizations used here,  $\alpha$  is independent of  $R$ . Not only does  $T / R^{0.46}$  vary with  $R$ , but so does  $\overline{h_i}(R)$  which we found to be given approximately by  $\overline{h_i}(R) = T / R^{0.46}$ . The value of  $\alpha$  varies by only about 10% even with extreme values for the reorientation definition parameters. The skewness for all of the data is 0.20 and the kurtosis for all data is 3.08, suggesting that the deviations from the average amplitude during reorientations are close to Gaussian.

An interesting relationship between  $\overline{h_i}$  and  $|j-j|$  for a full time series is revealed by their negative cross-correlation function

$$g_{hh}(\tau) = \frac{h(j_0(t)j_0(t+\tau)) - \overline{h_i}(R)\overline{h_i}(R)}{\sigma_h^2} \quad (1)$$

$$= \frac{h(j_0(t)j_0(t+\tau)) - \overline{h_i}(R)\overline{h_i}(R)}{\sigma_h^2} \quad (2)$$

$$= \frac{h(j_0(t)j_0(t+\tau)) - \overline{h_i}(R)\overline{h_i}(R)}{\sigma_h^2} \quad (3)$$

In Fig. 6 (a) we show  $g_{hh}(\tau)$  for  $R = 1:1 \cdot 10^0$ . The function  $g_{hh}(\tau) = a_0 \exp(-\tau/\tau_c)$  was fit to the data separately at each  $R$  to yield  $\tau_c^{g_{j0}}(R)$  and  $\tau_c^{g_{j1}}(R)$ . These time scales were made dimensionless by dividing the viscous diffusion time  $L^2/\nu$  by each of them, yielding Reynolds numbers  $Re^{g_{j0}} = L^2/\nu\tau_c^{g_{j0}}$  and  $Re^{g_{j1}} = L^2/\nu\tau_c^{g_{j1}}$ . These are plotted versus  $R$  in Fig. 6 (b). A power-law fit gives  $Re^{g_{j0}} = 0.41 R^{0.47}$  and  $Re^{g_{j1}} = 0.051 R^{0.46}$ . One sees that these two power laws have approximately the same exponent. This exponent value is found also for  $T$  [19], suggesting a close relationship between the different time scales of the problem. The time scale  $\tau_c^{g_{j1}}$  indicates how long the rotation rate and amplitude remain correlated, and it is about 80% of  $T$ . The time scale  $\tau_c^{g_{j0}}$  indicates by how much the amplitude leads the rotation rate. This is only about 6% of  $T$ , but the fact that the amplitude leads the rotation at all is remarkable, and suggests that an amplitude drop is a precursor of reorientations.

- [1] For instance, E. Siggia, *Annu. Rev. Fluid Mech.* 26, 137 (1994).
- [2] L. Kadano, *Phys. Today* 54, 34 (2001).
- [3] G. Ahlers, S. Grossmann, and D. Lohse, *Physik J.* 1, 31 (2002).
- [4] R. Krishnamurthy and L. N. Howard, *Proc. Nat. Acad. Sci. USA* 78, 1981 (1981).
- [5] M. Sano, X.-Z. Wu, and A. Libchaber, *Phys. Rev. A* 40, 6421 (1989).
- [6] B. Castaing, G. Gunaratne, F. Heslot, L. Kadano, A. Libchaber, S. Thomae, X.-Z. Wu, S. Zaleski, and G. Zanetti, *J. Fluid Mech.* 204, 1 (1989).
- [7] S. Ciliberto, S. Cioni, and C. Laroche, *Phys. Rev. E* 54, R5901 (1996).
- [8] X.-L. Qiu and P. Tong, *Phys. Rev. E* 64, 036304 (2001).
- [9] Y. Tsuji, T. Mizuno, T. Mashiko, and M. Sano, *Phys. Rev. Lett.* 94, 034501 (2005).
- [10] U. Hansen, D. Yuen, and S. Kroening, *Geophys. Astrophys. Fluid Dynamics* 63, 67 (1991).
- [11] S. Ciliberto, S. Cioni, and J. Sommeria, *J. Fluid Mech.* 335, 111 (1997).
- [12] J. Niemela, L. Skrbek, K. Sreenivasan, and R. Donnelly, *J. Fluid Mech.* 449, 169 (2001).
- [13] K. Sreenivasan, A. Bershadskii, and J. Niemela, *Phys. Rev. E* 65, 056306 (2002).
- [14] F. Fontenele Araujo, S. Grossmann, and D. Lohse, *arXiv preprint cond-mat/0407031v1* (2004).
- [15] E. van Doorn, B. Dhruva, K. Sreenivasan, and V. Casella, *Phys. Fluids* 12, 1529 (2000).
- [16] G. Glatzmeier, R. Coe, L. H ong, and P. Roberts, *Nature (London)* 401, 885 (1999).
- [17] E. Brown, A. Nikolaenko, D. Funfschilling, and G. Ahlers, *Phys. Fluids*, submitted.
- [18] C. Sun, H.-D. Xi, and K.-Q. Xia, submitted to *Phys. Rev. Lett.*
- [19] X.-L. Qiu and P. Tong, *Phys. Rev. Lett.* 87, 094501 (2001).